ELSEVIER

Seminars in
NUCLEAR
MEDICINE

[^{15}O]H_2O PET: Potential or Essential for Molecular Imaging?

Riemer H.J.A. Slart, MD, PhD,[*,†] T. Samara Martinez-Lucio, MD,[*] Hendrikus H. Boersma, PhD,[*] Ronald H. Borra, MD, PhD,[*] Bart Cornelissen, PhD,[*] Rudi A.J.O. Dierckx, MD, PhD,[*] Magdalena Dobrolinska, MD,[*,‡] Janine Doorduin, PhD,[*] Paola A. Erba, MD, PhD,[§] Andor W.J.M. Glaudemans, MD, PhD,[*] Bruno Lima Giacobbo, PhD,[*] Gert Luurtsema, PhD,[*] Walter Noordzij, MD, PhD,[*] Joyce van Sluis, PhD,[*] Charalampos Tsoumpas, PhD,[*] and Adriaan A. Lammertsma, PhD[*]

Imaging water pathways in the human body provides an excellent way of measuring accurately the blood flow directed to different organs. This makes it a powerful diagnostic tool for a wide range of diseases that are related to perfusion and oxygenation. Although water PET has a long history, its true potential has not made it into regular clinical practice. The article highlights the potential of water PET in molecular imaging and suggests its prospective role in becoming an essential tool for the 21st century precision medicine in different domains ranging from preclinical to clinical research and practice. The recent technical advances in high-sensitivity PET imaging can play a key accelerating role in empowering this technique, though there are still several challenges to overcome.
Semin Nucl Med 00:1-13

Introduction

Water is a key molecule that empowers life on our planet. Indeed, about 60% of the human body consists of water. It also is the main component of blood plasma and following the flow of water can provide information on perfusion. As blood flow may be altered in disease, imaging water may help to differentiate healthy from diseased tissue. Water can be imaged quantitatively using positron emission tomography (PET) together with tracer amounts of oxygen-15 labelled water ([^{15}O]H_2O).

[^{15}O]H_2O has characteristics that make it an ideal tracer for absolute quantification of blood flow (perfusion). Unlike many other tracers that are used as perfusion agents, such as [^{13}N]ammonia ([^{13}N]NH_3), Rubidium-82 chloride ([^{82}Rb]Cl) and [^{18}F]flurpiridaz, [^{15}O]H_2O is a freely diffusible and metabolically inert tracer. In addition, under normal and ischemic conditions, its extraction fraction is essentially

Abbreviations: AD, Alzheimer Disease; ASL, arterial spin labelling; BAT, Brown adipose tissue; BOLD, blood-oxygen-level-dependent; $CMRO_2$, cerebral metabolic rate of O_2 consumption; CAD, coronary artery disease; CBF, cerebral blood flow; CVD, cerebrovascular disorders; DBS, deep brain stimulation; DVT, deep vein thrombosis; fMRI, functional MRI; FOV, field-of-view; HD, Huntington's disease; IDIF, image derived input function; LAF, laminar flow; LAFOV, long axial field of view; LGE, Late Gadolinium Enhancement; MBF, myocardial blood flow; MCI, mild cognitive impairment; MDD, Major Depressive Disorder; MDR, Medical Device Regulations; OEF, oxygen extraction fraction; PAD, peripheral arterial disease; PD, Parkinson's disease; PET, positron emission tomography; PET-MRI, positron emission tomography-magnetic resonance image; PTF, perfusable tissue fraction; PTI, perfusable tissue index; PTSD, post-traumatic stress disorder; PVD, peripheral vascular disease; SPECT, single photon emission computed tomography; TBF, tumor blood flow

*Department of Nuclear Medicine and Molecular Imaging, Medical Imaging Center, University Medical Center Groningen, University of Groningen, Groningen, The Netherlands.
†Department of Biomedical Photonic Imaging, Faculty of Science and Technology, University of Twente, Enschede, The Netherlands.
‡Department of Cardiology and Structural Heart Diseases, Medical University of Silesia, Katowice, Poland.
§Department of Medicine and Surgery, University of Milan Bicocca, and Nuclear Medicine Unit ASST Ospedale Papa Giovanni XXIII, Bergamo, Italy.
Address reprint requests to Riemer H.J.A. Slart, MD, PhD, Department of Nuclear medicine & Molecular Imaging (EB50), University of Groningen, University Medical Center Groningen, Medical Imaging Center, Hanzeplein 1, PO 9700 RB, Groningen, The Netherlands. E-mail: r.h.j.a.slart@umcg.nl

https://doi.org/10.1053/j.semnuclmed.2023.08.002

100%, which means that the rate of $[^{15}O]H_2O$ uptake in tissue is linearly related with actual blood flow, whereas this relationship is non-linear for metabolically trapped tracers.

Oxygen-15 has a short half-life of 122 seconds, resulting in short scan protocols and a relatively low overall radiation burden. Consequently, a $[^{15}O]H_2O$ scan can easily be added to scan protocols with other established or novel tracers. This provides the possibility to correct uptake of those other tracers for flow effects. Quantification is reasonably easy using relatively straightforward kinetic analysis of dynamic PET data, with a typical scanning duration of 5 to 10 minutes. On the other hand, due to the short half-life of oxygen-15, an onsite cyclotron is needed for its production. Ideally, this should be a dedicated (small size) cyclotron in order to ensure optimal availability and minimal impact on the production of other PET tracers within the same facility.

Perfusion imaging using $[^{15}O]H_2O$ PET is increasingly being used by many centers throughout Europe, especially for myocardium imaging. At present, $[^{15}O]H_2O$ is not approved by the Food and Drug Administration limiting its clinical use in the United States of America. Under the Medical Device Regulations (MDR) in Europe, combined with cGMP regulations, its use is possible. With the emergence of digital PET and long axial field-of-view (LAFOV) PET, also referred to as "Total Body PET," dynamic imaging of $[^{15}O]H_2O$ across large anatomical areas and organ systems within a single scan has become feasible. As LAFOV PET enables the measurement of the image derived arterial input function without having to insert an arterial cannula, use of $[^{15}O]H_2O$ is expected to continue to expand within both research and clinical applications providing comprehensive information for more accurate diagnosis, precision therapy evaluation and other applications.

The purpose of this review is to outline and dissect current opportunities and challenges for $[^{15}O]H_2O$ PET, including those related to its practical implementation, together with business and financial aspects that may be relevant when setting up $[^{15}O]H_2O$ PET at a nuclear medicine department (Table 1).

History

The use of $[^{15}O]H_2O$ to measure blood flow was first reported by Ter-Pogossian et al.[1] Originally, the technique was developed for the brain and, as no tomographic techniques were available, detection sensitivity decreased with the depth in tissues and recorded values of flow represented mixtures of grey and white matter.[2,3]

Following the introduction of quantitative PET,[4] there was renewed interest in the use of both $[^{15}O]H_2O$ and $[^{15}O]O_2$ to measure perfusion and oxygen metabolism, respectively. Unfortunately, due to movement of detectors during a scan, the first generation of commercial PET scanners[5] was not suitable for dynamic scanning and, therefore, use was made of the oxygen-15 steady state inhalation technique.[6] In this method blood flow is measured during continuous inhalation of $[^{15}O]CO_2$, which essentially is the same as a continuous infusion of $[^{15}O]H_2O$ due to the catalytic effect of carbonic anhydrase in the pulmonary capillaries.[7] A full description of its implementation for PET together with preliminary results in healthy volunteers was provided by Frackowiak et al.[8] A few years later, an alternative technique based on intravenous injection of $[^{15}O]H_2O$ was developed by Herscovitch et al.[9] and Raichle et al.[10] This so-called autoradiographic method was based on a method originally developed by Kety.[11]

In these early methods, the volume of distribution of water had to be fixed, as the use of a single static scan allowed for estimation of only a single parameter. Currently, nearly all $[^{15}O]H_2O$ studies are based on dynamic scanning, and when necessary, accompanied with simultaneous sampling of the arterial plasma input function, providing more accurate quantification of both blood flow and volume of distribution of water.[12]

Logistics and Workflow

Oxygen-15 with a half-life of 122 seconds is produced with a cyclotron. Due to its short half-life, it is crucial to optimize

Table 1 Advantages and Challenges of $[^{15}O]H_2O$ PET Studies

Advantages	Challenges
Very low radiation burden (ie, 100-500 μSv)	Needs a lot of operational time of a conventional cyclotron, so a dedicated cyclotron for ^{15}O-water production is preferable
Fast dynamic imaging (ie, 6-10 minutes)	More expensive than other methods (e.g., SPECT, comparable MRI methods)
Approved for local clinical use in several countries	Moderate image quality due to positron range, including gating
Superior quantification methods compared with other methods (eg, SPECT, MRI, CT, $[^{13}N]NH_3$ or ^{82}Rb PET)	Clinical and preclinical scanners preferably are connected to an efficient dose delivery system
CE marked software available	Needs arterial cannulation for arterial input function if the heart or a large artery is not within the field-of-view
High heart-to-background contrast	
Metabolically inert, freely diffusible (ideal)	
Long axial field-of-view PET allows many more opportunities	

logistics of production and scanning, and to have the cyclotron in close proximity of the scanner room.

There are several methods to produce oxygen-15 with a cyclotron, the most often used is taking oxygen-15 in the chemical form of the preproduced $[^{15}O]O_2$ gas as the starting material and then convert it to $[^{15}O]H_2O$. The first description of $[^{15}O]H_2O$ production can be found in Clark and Buckingham (1975), and in work of 1976 by the research groups of Welch.[13,14] The production was performed using a cyclotron that accelerates deuterons in combination with a low energy beam. To produce ^{15}O via deuteron acceleration, the target must be filled with a mixture of highly purified nitrogen gas and a trace of oxygen gas. Because of this relatively cheap starting gas mixture, this procedure is suitable for a pass-through gas target, enabling continuous production of $[^{15}O]H_2O$. A detailed description of this process is provided by Clark et al.[15] The book "short-lived radioactive gases for clinical use" by Clark and Buckingham describes a complete overview of ^{15}O radionuclide development processes.[14]

A recent publication has brought attention to the eventual microbiological risks of radiopharmaceuticals, as their self-sterilization potential is absent. This means that also the microbiological risk of the instant production of $[^{15}O]H_2O$ needs to be investigated in a systematic way in order to minimize any microbiological risks.[16]

One of the solutions to address microbiological risks in combination with continuous $[^{15}O]H_2O$ production is to use an examination room based device that has a fully disposable and quickly replaceable sterile injection system, with inline 0.22 μm filters, valves and diffusion chamber next to the patient, such as the Hidex radioactive water generator system (Hidex Oy, Turku, Finland) which is also compatible with the presence of high magnetic fields.[17] Such a bedside system not only allows for rapid patient flow, as little time is needed to make the system ready for the next patient / injection, but also allows for simultaneous monitoring of both bolus shape and total delivered $[^{15}O]H_2O$ dose to the patient, in turn improving repeatability of the overall $[^{15}O]H_2O$ bolus shape. Such a system requires the direct communication of the injector and monitoring system with a cyclotron. Another system with a similar bedside philosophy, yet also incorporating the entire tracer production at the bedside, in contrast to the previous system, is the MedTrace system (MedTrace, Hørsholm, Denmark).[18]

The introduction of medical cyclotrons designed for high yield ^{18}F-production, and thus proton only cyclotrons, had a significant boost on the production of oxygen-15.[19] Consequently, the production of $[^{15}O]H_2O$ has changed from continuous to bolus for sites, as an alternative route to the necessity for a dedicated (mini-)cyclotron for oxygen-15 production. For example, the $[^{15}O]H_2O$ bolus production at our department (University Medical Center Groningen, Groningen, the Netherlands) makes use of an 18 MeV cyclotron from IBA (IBA Radiopharma Solutions, Vlaams-Brabant, Belgium) which accelerates hydrogen anions and converts them into cations (ie, protons) by stripping the 2 electrons. Bombardment with protons to nitrogen gas target initiates the nuclear reaction: $^{15}N(p,n)^{15}O$. The target gas enrichment is higher than 99% $[^{15}N]N_2$ with only a trace amount of O_2 to a ratio of 39:1 v/v (Isotec Inc, obtained through Campro Scientific, Veenendaal, The Netherlands).

The product of the nuclear reaction is $[^{15}O]H_2O$ in gas form. This is transferred to a specific module where it is mixed with hydrogen gas and passed through a palladium column heated up to 150 °C. The $[^{15}O]H_2O$ production module contains a disposable sterile cartridge, in which the produced $[^{15}O]H_2O$ is collected and mixed with a sterile 0.9% saline solution to obtain a final product suitable for patient administration. The sterile cartridge needs to be assembled before installation within the module. To guarantee a sterile product, the entire lead shielded module is placed within a Class A laminar flow (LAF) cabinet, and for $[^{15}O]H_2O$ this is checked afterwards due to its short half-life.

Finally, in addition to automated (bedside/other) systems which help standardize the $[^{15}O]H_2O$ bolus delivery, it is important to note that having reliable, validated and regulatory approved software packages are essential to deploy $[^{15}O]H_2O$ reliably in clinical practice. Given the benefits of $[^{15}O]H_2O$, especially for assessment of myocardial perfusion, well-known software packages are available for $[^{15}O]H_2O$ water studies in this area, such as the Carimas, aQuant, and Cardiac Vuer.[20-22]

Preclinical

Small animal imaging is a useful resource to understand health and disease, and treatment mechanisms in mammals. Preclinical PET offers the advantage of studying the same molecules in animals before using these in humans. This is also the case with $[^{15}O]H_2O$, however, there are some practical limitations and difficulties to perform such scans. Within these, the very short half-life of ^{15}O makes very close proximity to a cyclotron a necessity. Although clinical installations may be designed with this in mind, preclinical imaging facilities often do not make use of $[^{15}O]H_2O$ PET as it is seen as too complex.[23] Nevertheless some scientists have warm interest in studying the biological response to $[^{15}O]H_2O$. For example, the SAFIR collaboration in Zurich has dedicated a lot of resources to build a pioneering PET insert for preclinical PET -magnetic resonance image (PET-MRI) that aims to allow measuring relatively high injected dose (eg, 500 MBq) of $[^{15}O]H_2O$ with short frames (up to 5 s) and high resolution (ie, 2 mm) for at least 10 minutes after its injection in order to study the rat brain with higher detail than ever before.[24]

Brain Applications

$[^{15}O]H_2O$ brain PET in a preclinical setting has mostly been used to study cerebral perfusion in rats. In animal models of stroke, $[^{15}O]H_2O$ PET was successfully used to measure changes in perfusion after occlusion of the middle cerebral artery[25-29] or anterior cerebral artery.[30] For example, Martín et al.[25] showed hypoperfusion during middle cerebral artery occlusion followed by reperfusion immediately after the

occlusion was released. Then, hypoperfusion could be observed at days 1 and 2, and hyperperfusion at days 4 and 7.

While [^{15}O]H_2O PET has widely been used to study brain activation in humans, such studies in rats are limited. Wehrl et al.[31] studied brain activation after whisker stimulation using [^{15}O]H_2O PET and compared the findings with blood-oxygen-level-dependent (BOLD) functional MRI (fMRI) measurements. Interestingly, it was shown that the intensity, shape and location of the [^{15}O]H_2O PET signal differed from that of the BOLD-fMRI response. As the physiological basis of BOLD-fMRI is not completely understood, this highlights the potential role of [^{15}O]H_2O PET in studying brain activation complementary to fMRI.

Cardiovascular Applications

Preclinical assessment of myocardial blood flow (MBF) using [^{15}O]H_2O has predominantly been used in pigs and dogs and less frequently in rodents. In some of the earlier studies, [^{15}O]H_2O PET was validated by comparing measured MBF results with microsphere data. These (ischemic) animal models were useful for cardiac validation and repeatability studies, mainly applied with the single-tissue-compartment model, and sometimes including the perfusable tissue fraction (PTF), which provides a quantitative MBF value that is more robust to partial volume effects. Past research has shown that values of [^{15}O]H_2O correlate consistently with microsphere data, and that the inclusion of PTF could help to identify both tissue perfusion and viability with [^{15}O]H_2O.[32-37] When compared to quantification with other PET radiotracers available for blood flow (eg, [^{13}N]NH_3), water shows the best correlation to microspheres quantification, confirming the absolute correlation of [^{15}O]H_2O perfusion with MBF.[38,39]

Oncology Applications

[^{15}O]H_2O concentration shows a linear relationship with signal intensity as measured with PET, particular at short acquisition time, which reflects tissue perfusion. Therefore, this technique is able to absolutely quantify tumor perfusion.[40] However, only a very limited number of small animal studies have been reported using [^{15}O]H_2O for the assessment of tumor blood flow.[41,42]

As discussed earlier, there is a perceived lack of small animal-studies, which reason may be twofold. The relatively long positron range of ^{15}O (R_{mean} = 3.0 mm), compared to other PET radionuclides such as ^{18}F. As usually tumors growing in mice are less than 1 cm wide, it makes [^{15}O]H_2O PET less ideal, with large partial volume effects, potentially invalidating quantitative methods.[43]

Clinical Applications

Clinical PET/CT imaging is a key resource to evaluate the (patho)physiological processes underlying some of the most important diseases in the human body. PET/CT offers the advantage of adding information about the physiology on top of the anatomical evaluation. Particularly with [15O]H_2O, there is the possibility to truly quantify absolute and regional blood flow supply to different organs, as this tracer has a perfect linear relationship with the arterial circulation. This opens up an opportunity of evaluating diverse organs for a wide variety of pathological processes, as differences in the hemodynamic status of tissues have been described between healthy and unhealthy states.

Brain Applications

In the brain, [^{15}O]H_2O PET can provide valuable insights in cerebral hemodynamic changes under healthy (eg, aging, task-based activities) and diseased (eg, neurodegenerative diseases, psychiatric disorders) conditions. Cerebral metabolic rate of O_2 consumption ($CMRO_2$), cerebral blood flow (CBF), and the balance between those 2, that is, oxygen extraction fraction (OEF), are important indicators of possible disease related changes in brain function[44] with [^{15}O]H_2O being a reliable method to measure CBF.[45,46] An example of [^{15}O]H_2O brain PET scan from a healthy volunteer is depicted in Fig. 1.

In a pathophysiological context, many diseases in the brain are highly associated with changes in CBF, either being the main manifestation of the underlying pathophysiological process of a disease, such as the case of cerebrovascular disorders (CVD) or playing a secondary—but still important—role in disease onset and progression. In a study from Scarmeas and colleagues, CBF was negatively associated with overall cognitive reserves and worse prognosis for Alzheimer's disease (AD).[47] In another study, Xu and colleagues assessed CBF using both [^{15}O]H_2O and arterial spin labelling (ASL) imaging. They reported a significant age-related decrease in CBF in patients with mild cognitive impairment (MCI). AD patients showed an even more pronounced decrease in CBF when compared with their control counterparts, suggesting a significant effect of AD in the CBF.[48] These findings confirm the possibility of using CBF measurements as a biomarker for diagnosis of AD but this may also function as a biomarker to observe early signs of the disease.[49,50] Although AD is the most studied neurodegenerative disorder, other ones such as Parkinson's disease and Huntington's disease (PD and HD, respectively) also showed altered blood flow comparable to a reduced metabolic activity in cortical and subcortical areas of the brain.[51-54] Therefore, CBF change clearly plays a key role in neurodegenerative disorders, although it is not clear to what extent such modifications would lead to disease onset or hasten disease progression. On that note, it is possible that [^{15}O]H_2O PET can provide another method to assess disease onset and progression in a neurodegenerative context, especially when used in combination with other imaging techniques.

Another possible use of [^{15}O]H_2O PET is the assessment of blood flow in psychiatric conditions. [^{15}O]H_2O has been used in many psychiatric disorders, with CBF being highly variable on a disease-dependent basis. Studies in Major Depressive Disorder (MDD) have shown significantly

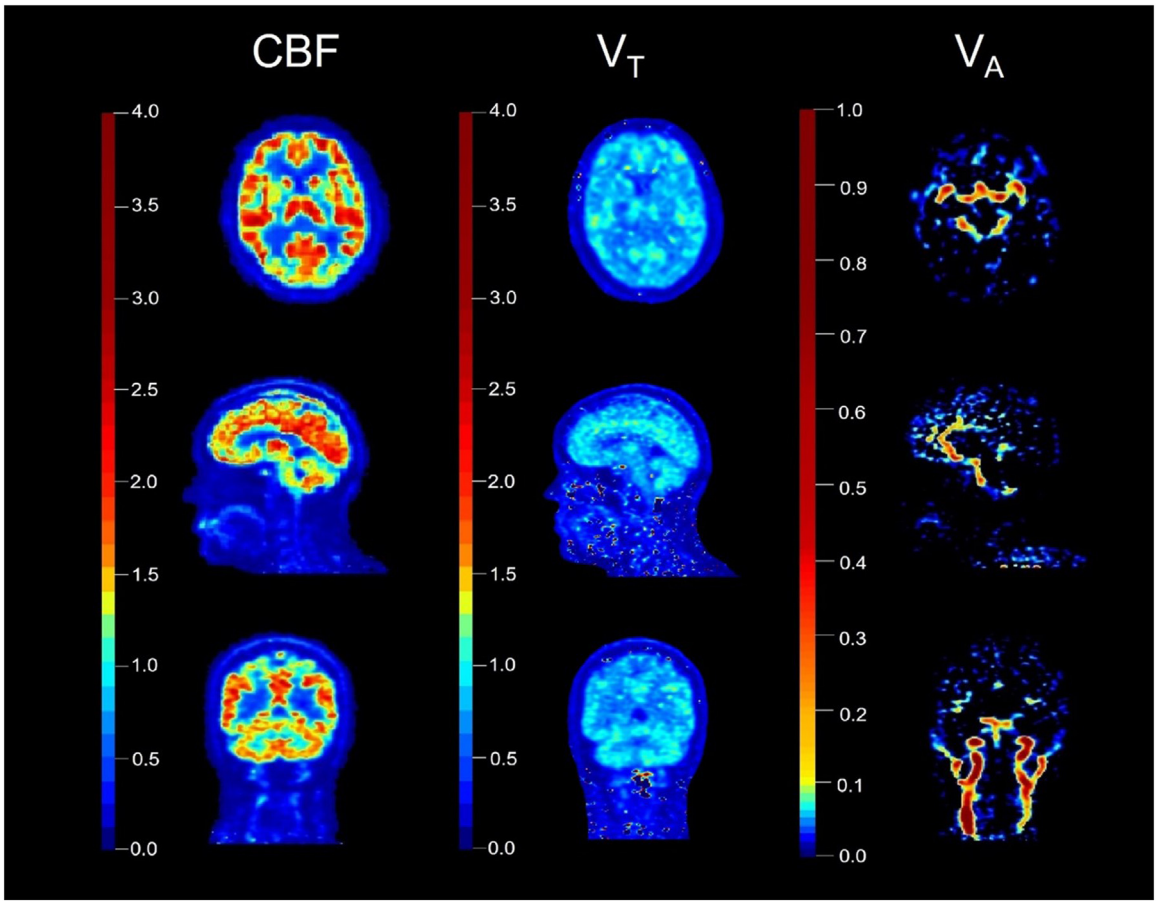

Figure 1 Single-tissue compartment model parametric brain images with $[^{15}O]H_2O$ PET from a healthy volunteer from left to right the images correspond to cerebral blood flow (CBF ml·min^{-1}·g^{-1}), volume of distribution (V_T - mL·cm^{-3}) and arterial blood volume (V_A - mL/g). From top to bottom transaxial, sagittal, and coronal slices. In general, CBF illustrates the influx into grey matter (mainly shown with red and orange) and V_T exhibits the ratio between the tracer concentration in the target tissue (light blue). In the transaxial planes CBF, the caudate nucleus and posterior limb of internal capsule can be identified mainly in red or yellow, respectively. In the same plane of V_A is depicted part of the cerebral arterial circle (Willis), anterior communicating artery in the joint of the anterior cerebral left and right arteries and left and right posterior cerebral arteries. In the sagittal plane of CBF and V_T can be identified in red and yellow (CBF) and light blue (V_T), respectively, the thalamus. In the sagittal plane of V_A can be distinguished the internal carotid artery in its cavernous portion. In the coronal plane can be observed in red and yellow from the CBF, the corpus callosum. Finally, in the coronal plane of V_A can be recognized the right and left common carotid arteries and their bifurcations into external and internal carotid arteries.

decreased blood flow in the posterior cingulate, insula, orbitofrontal cortex, and temporal cortex.[55,56] Regarding depression disorder, Dunn and colleagues reported a lack of correlation between blood flow and glucose metabolism in unipolar depression patients, a behavior not observed in patients with bipolar disorder, even when both groups of patients were clinically stable and on fixed-dose medication for at least 3 months.[55] To assess whether changes in CBF could be observed after treatment, 1 study assessed the effects of deep brain stimulation (DBS) on CBF using $[^{15}O]H_2O$ PET in patients with treatment-refractory depression. The authors reported a significant CBF increase in prefrontal cortex in subjects submitted to DBS with significant symptom improvement compared with non-responders, and the increase in CBF remained after discontinuation of stimulation, suggesting long-lasting effects of DBS.[57] In anxiety-related disorders, the main use of $[^{15}O]H_2O$ PET was to assess CBF in post-traumatic stress disorder (PTSD). Two studies showed a significant change in $[^{15}O]H_2O$ PET signal in the prefrontal cortex, cingulate cortex, insular cortex, amygdala and hippocampus that correlated with adrenocorticotropic hormone in combat veterans with PTSD when compared to age-matched controls.[58,59] One study compared blood flow in healthy controls, and combat veterans with and without PTSD. $[^{15}O]H_2O$ PET imaging showed differences in CBF between healthy controls and both combat veteran groups when all groups were exposed to an aversive stimulatory event during the scan. Interestingly, combat veterans with PTSD had altered neural responses in the medial prefrontal cortex and amygdala when compared with veterans without PTSD, suggesting disease-specific activation and change in blood flow in these specific regions.[60] These results

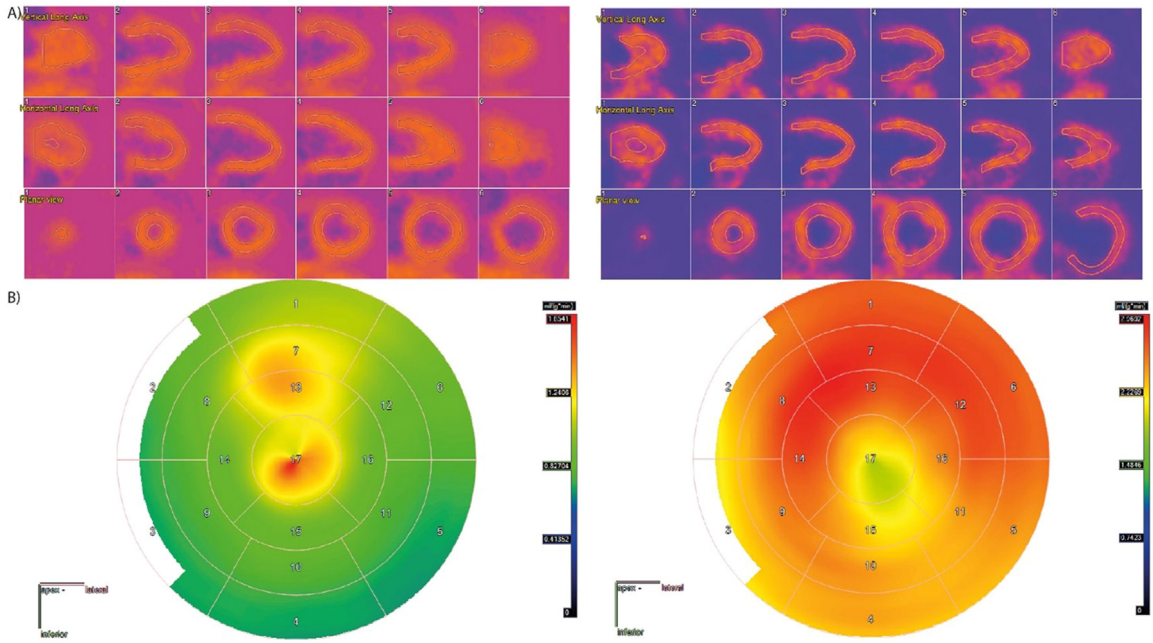

Figure 2 Representative rest and adenosine stress myocardial perfusion by [^{15}O]H_2O PET (A) The figure shows vertical long axis, horizontal long axis, and short axis of rest (left) and adenosine stress (right) myocardial perfusion. (B) 17-segments polar maps of stress rest (left) and stress (right) myocardial perfusion.

show the current use of [^{15}O]H_2O PET for measurement of CBF in psychiatric disorders and, although not fully explored, opens the possibility of observing the changes of blood flow during the course of a treatment. Additionally, [^{15}O]H_2O PET may be able to map different disease patterns that may be interesting in the basic understanding of psychiatric disorders and may contribute to devise a more individualized and precise treatment protocol for these neurological disorders.

In summary, there is a wide range of possibilities for using [^{15}O]H_2O PET imaging both for a better comprehension of the healthy brain,[61] but also as a possible imaging marker for brain disorders. In combination with other PET tracers such as [^{18}F]fluorodeoxyglucose ([^{18}F]FDG), or other imaging modalities such as MRI, it might be possible to map different brain patterns, and improve diagnosis and treatment accuracy.[62]

Cardiovascular Applications

In nuclear cardiology, [^{15}O]H_2O is considered the gold standard for quantification of MBF.[63,64] In fact, other well-established tracers available for quantification of MBF, that is, [^{13}N]NH_3 and [^{82}Rb]Cl, have been validated against [^{15}O]H_2O. Since [^{15}O]H_2O is freely diffusible across capillary and cell membranes, has an extraction fraction of essentially 100%, and is metabolically inert, it is the ideal tracer for MBF measurements along the entire spectrum of coronary artery disease (CAD). However, as it is not (metabolically) retained in tissues, voxel-based kinetic modelling is time consuming and sensitive to noise. Nevertheless, since the basis function method of the single-tissue compartment model, incorporating right ventricle spill-over, was implemented, it has been possible to automatically generate parametric images of absolute MBF in only a short time frame.[65] An example of parametric images from myocardial perfusion imaging by [^{15}O]H_2O PET is given in Fig. 2, complemented by their corresponding values in Table 2.

According to data from the PACIFIC trial, [^{15}O]H_2O PET had higher accuracy for detecting myocardial ischemia than CT and myocardial scintigraphy.[66] In addition, combining [^{15}O]H_2O PET derived MBF with anatomical features such as CT derived coronary artery stenosis severity and plaque morphology, produces the highest prognostic value for all-cause mortality and myocardial infarction.[67] After successful revascularization of the coronary arteries in patients with CAD, [^{15}O]H_2O PET derived MBF significantly improved along with improved fractional flow reserve.[68]

Myocardial viability has been successfully assessed from different [^{15}O]H_2O PET derived parameters, such as reduced resting MBF, PTF, and perfusable tissue index (PTI), in various experimental models against MRI.[69] PTI and PTF have been used to successfully predict (near) transmural Late Gadolinium Enhancement (LGE) on MRI, with LGE in turn serving as an (imperfect) surrogate marker of myocardial viability. Furthermore, the fast kinetics of [^{15}O]H_2O allows for shorter scanning time, and real-time measurement of MBF during exercise (eg, with the use of a bicycle/ergometer) positioned appropriately inside the PET scanner as a way to avoid the use of pharmacologically induced stress (eg, using adenosine or regadenoson).[70]

Finally, the use of [^{15}O]H_2O PET-MRI in the heart has the potential to combine cardiac perfusion imaging with a library of sequences commonly used in cardiac MRI (eg, ejection fraction, intravascular flow measurements, tissue characterization).[71,72]

Table 2 Myocardial Blood Flow (MBF) in Stress and Rest Phase, Myocardial Flow Reserve (MFR), and Perfusable Tissue Index (PTI) Corresponding to Figure 2

Segment	MBF Rest (mL/g/min)	MBF Stress (mL/g/min)	MFR (mL/g/min)	PTI Rest	PTI Stress
1	1.0	2.7	2.7	0.61	0.65
2	0.8	2.3	2.9	0.78	0.78
3	0.7	2	2.8	0.85	0.73
4	0.7	2.4	3.4	0.77	0.59
5	0.7	2.4	4.3	0.79	0.71
6	0.9	2.7	3.0	0.64	0.72
7	1.3	2.9	2.2	0.57	0.75
8	0.9	2.7	3.0	0.70	0.82
9	0.8	2.5	3.1	0.79	0.83
10	0.8	2.4	3.0	0.81	0.71
11	0.7	2.4	3.4	0.80	0.71
12	0.9	2.9	3.2	0.73	0.87
13	1.3	2.7	2.1	0.61	0.78
14	0.9	2.8	3.1	0.71	0.81
15	0.9	2.2	2.4	0.76	0.64
16	0.9	2.4	2.7	0.77	0.75
17	1.3	2.1	1.6	0.71	0.66

Miscellaneous: Tissue, Limb, and Organ Perfusion

Peripheral vascular disease (PVD) is an entity caused by dysfunction in the circulatory system, which results from damage, occlusion and/or inflammation of arteries and/or veins, excluding brain and heart vasculature. Most relevant diseases encompassed under the PVD umbrella include peripheral arterial disease (PAD), chronic venous insufficiency (CVI), and deep vein thrombosis (DVT).[73] PAD is an atherosclerotic disease that, when affecting the lower extremities, results in skeletal muscle ischemia, intermittent claudication, and, in more severe stages of disease, limb amputation and death. Several techniques have been used for the evaluation and detection of PVD, including ankle–brachial indices, duplex ultrasound, MRI, CT angiography, single photon emission computed tomography (SPECT), and PET. The ankle-brachial index is a widely applied diagnostic tool for the detection of PAD that uses the blood pressure differential between upper and lower extremities to detect a functionally significant arterial obstruction, but this technique can be problematic in the setting of microvascular disease and medial calcification. In vivo nuclear imaging approaches provide high sensitivity and, when using biologically targeted radiotracers, potentially offer novel methods for the investigation of PAD, with integration of perfusion and assessment of tissue oxygenation, metabolism, or biologic processes such as angiogenesis.[74] $[^{15}O]H_2O$ PET is useful for repeated measurements of blood flow in the same individual during a single scan session, at rest and during exercise, or during vasodilator stress.[74-76] A $[^{15}O]H_2O$ rest-stress PET study found significant differences in flow reserve within the calves of PAD patients when compared with healthy volunteers, and these differences correlated with thermodilution-derived flow reserve values.[77] Another study found significantly reduced exercise-induced muscle blood flow in the distal legs of PVD patients who were referred for lower-limb amputation, suggesting that $[^{15}O]H_2O$ PET imaging may be a valuable tool for determining the level of subsequent amputations.[78] Kalliokoski et al. demonstrated that PET assessment of skeletal muscle blood flow and oxygen uptake in lower-extremities may be a useful tool for evaluating patient responses to exercise training programs.[79] Apart from assessing (skeletal) muscle, $[^{15}O]H_2O$ PET imaging has also been applied in the field of tendon studies in athletes during rest and during exercise.[80]

Another field of interest is quantification of regional liver and splenic blood flow, where dynamic $[^{15}O]H_2O$ PET shows promise for clinical use.[81,82] Different factors make accurate estimation of liver blood flow difficult, such as the dual blood flow supply (hepatic artery and portal vein), inaccessibility of the portal vein for direct flow measurements, and changes in extraction kinetics in the pathological liver.[83] Despite these difficulties, standardized and routine quantification of liver blood flow could translate into advances in personalized therapies in patients with distinct hepatic insults. Also, splenic blood flow could be important in the analysis of regional hemodynamic of the spleen in patients with hypersplenism, portal hypertension, after traumatic spleen rupture, and in various other conditions.

Brown adipose tissue (BAT) has emerged as a potential target to combat obesity and diabetes, but novel strategies to activate BAT are needed. PET with $[^{15}O]H_2O$ has been evaluated for direct measurements of adipose tissue perfusion,[84] resulting in a positive correlation with glucose uptake in obese and nonobese healthy subjects, as well as in patients with diabetes, including medical drug response monitoring.[85] Adenosine administration caused a maximal perfusion effect in human supraclavicular BAT, indicating increased oxidative metabolism.[86]

Oncology Applications

One of the first applications of using [^{15}O]H_2O PET was to visualize cerebral tumors by measuring the regional cerebral blood flow together with oxygen utilisation.[87] Furthermore, the first application of [^{15}O]H_2O PET outside the brain in oncology was the measurement of regional blood flow (in combination with oxygen utilization and blood volume) in patients with breast carcinoma.[88]

Angiogenesis, the process in which new blood vessels originate from existing vasculature, is essential for tumor growth, progression, and development of metastases,[89,90] leading to increased blood flow in the tumor. Imaging of tumor blood flow (TBF) for tumor characterization and treatment response monitoring has therefore been studied in various cancers, such as non-small cell lung cancer,[91,92] colorectal cancer,[92,93] breast cancer,[94,95] head and neck cancer,[96] prostate cancer,[97] and brain cancer.[98] The field of cancer drug development would benefit from quantification of the vascular characteristics in tumors to assess the effectiveness of antiangiogenic agents, particularly the combination of [^{15}O]H_2O with another PET tracer.[99] For example, antiangiogenic treatment was expected to normalize perfusion and therefore improve delivery of chemotherapy. However, a research group from Amsterdam found that reduction in radiolabeled docetaxel uptake was due to a reduction in perfusion after bevacizumab as shown by a combined [^{15}O]H_2O and ^{11}C-Docetaxel PET scan.[99]

The gold standard for (minimally invasive or even in some cases completely noninvasive) quantitative measurements of TBF is [^{15}O]H_2O parametric PET[93] and these measurements can be performed with high reproducibility.[90,100,101] Using conventional PET systems with an axial field-of-view (FOV) of 15 cm to 25 cm,[102] an image derived input function (IDIF) for noninvasive TBF quantification can only be obtained for studies where the heart is in the (restricted) FOV, except for a recent generation of scanners with dedicated bed motion protocols allowing scanning of the heart area during a critical phase after the injection and also covering the target anatomy, such as multiparametric PET technology.[103] This limitation is resolved by the recent introduction of LAFOV PET,[104-106] where the heart together with all main organs and regions of interest can be captured in a single view, ensuring that an IDIF is also possible for structures further away from the heart. The use of an input function measured from the blood pool has been validated successfully in the past for cardiac studies[65] and also for the brain by Iida et al. who combined 2 PET scanners to simultaneously image the brain and the heart in a single scanning session.[107] Consequently, LAFOV dynamic scans allow acquisition of TBF information for multiple lesions within the FOV, which is important in case of intertumor heterogeneity. Given known associations of tumoral heterogeneity and resistance to targeted precision therapy, capturing all lesions simultaneously is important for response monitoring,[108] as overall patient response depends on the response of the poorest lesion.[102]

Multitracer Imaging

The short radioactive half-life of oxygen-15 (122 s) together with the corresponding relatively low radiation exposure allows for repeated [^{15}O]H_2O PET acquisitions at 10 min intervals. This, in turn, provides the possibility to directly measure short-term therapy effects in a single imaging session. Alternatively, a second scan can be performed using a different tracer for further characterization of, for example, tumor biology.[40] The use of more than 1 tracer in 1 scanning session has not been uncommon in clinical research. For example, at Hammersmith Hospital a usual scanning protocol involved imaging human participants with [^{15}O]H_2O to measure cardiac perfusion, inhaled [^{15}O]CO to measure blood volume and [^{18}F]FDG to measure cardiac viability and metabolism. The 3 different types of information were used to extract specific biological parameters to study hyperinsulinism in humans.[109]

The advantage of fast decaying [^{15}O]H_2O makes it a unique radiotracer suitable for use in dual or even triple tracer PET imaging in 1 session. In particular, the use of [^{15}O]H_2O PET imaging would be greatly enhanced once it is routinely possible to accurately separate the signal of [^{15}O]H_2O and another radiotracer once the 2 tracers are injected in the human body at the same time. It has been demonstrated to be feasible to separate the signal of multitracer scanning of a single [^{18}F]FDG and 6 consecutive [^{15}O]H_2O bolus injections.[110] This approach could allow [^{15}O]H_2O to measure how much uptake of a coinjected tracer (eg, [^{18}F]FDG or ^{89}Zr-labelled monoclonal antibodies) is related to changes in perfusion.

Implementation

Validation and Radiation Dose

A fundamental advantage of [^{15}O]H_2O used for PET imaging is the ultra-low radiation dose of only 1.2 μSv·MBq^{-1} that is delivered to a person.[111] This corresponds to a dose as low as approximately 500 μSv for standard PET scanners, which could be meaningfully lowered even further with highly efficient state-of-the-art (ie, LAFOV) PET scanners, as already demonstrated with [18F]FDG.[112] Furthermore, the development of CT scanners with appropriate filters and acquisition parameters can allow to achieve an ultra-low CT dose (ie, less than 100 μSv),[113] and this would make it possible to use [^{15}O]H_2O PET/CT as an imaging technique to scan even healthy young volunteers for obtaining "health-related knowledge," as of today, pathophysiological knowledge is "biased" as nuclear imaging techniques are performed only in patients with strict clinical indications due to radiation burden concerns. The fact that ultralow dose combined PET and CT can approach the natural background radiation levels could potentially permit the utilization of PET for measuring the perfusion of the embryo in utero.[114] This could offer new insights regarding the perfusion in the materno-placental-fetal system, and could allow the detection of significant abnormalities in the development of the embryo's organs at

very early stages swiftly guiding clinicians to either intervention or termination of pregnancy.[114]

Challenges and Future Perspectives

The inert PET tracer $[^{15}O]H_2O$ represents the accepted gold standard for absolute quantification of tissue perfusion in myocardium, brain and other variety of pathological conditions including cancer. Multiple obstacles thus far have blocked the routine use of PET perfusion imaging, including dependence of a cyclotron, image processing, clinical standardization, regulatory approval, reimbursement, and feasible clinical workflows.[64,115] Fortunately, some of these obstacles have been overcome, especially with the introduction of mini cyclotrons opening the door for PET perfusion imaging to become standard clinical practice in more centers around the world. In the foreseeable future, it is possible that LAFOV PET perfusion imaging with $[^{15}O]H_2O$ will be able to be performed in a single imaging session concurrent with standard PET imaging techniques such as $[^{18}F]$FDG PET. This approach could establish an efficient clinical workflow making $[^{15}O]H_2O$ PET a valuable tool for better patient management especially when patients are scanned with LAFOV PET, where arterial cannulation would be avoided, allowing a "true" noninvasive approach. These scanners can measure brain and heart perfusion, organ crosstalk, and absolute tumor blood flow quantification in combination with glycolysis, which will provide important complementary information regarding the prognosis, treatment adequacy, and therapy response.

Furthermore, the application in the context of LAFOV can allow for extending brain activation studies across the linked organ axes / connected body systems, something that is simply not possible with current fMRI technologies.

Future developments in PET-MRI may allow for maximizing the synergistic benefits of PET and MRI in the context of PET reconstruction, including positron range reduction[116] and more advanced PET image reconstruction utilizing information from MRI.[117] Furthermore, simultaneous PET-MRI could potentially offer motion compensation, which is important for more accurate kinetic analysis.[118]

Conclusion

$[^{15}O]H_2O$ PET has been well established in various domains of molecular imaging and particularly in myocardial perfusion. Although many significant advantages, such as the miniscule radiation burden and absolute quantification of perfusion, several challenges remain before transforming $[^{15}O]H_2O$ PET from a potential to an essential worldwide-spread tool in the clinical routine and research.

Author Contributions

Riemer H. J. A. Slart: Conception and design of the work, data collection for the introduction, preclinical cardiovascular applications, clinical cardiovascular applications, clinical miscellaneous applications, challenges and future perspectives, drafting of the manuscript, critical revision of intellectual content, and final approval of the manuscript; T. Samara Martinez-Lucio: Design of the work, data collection for clinical brain applications, conclusion, drafting of the manuscript, critical revision of intellectual content, and final approval of the manuscript; Hendrikus H. Boersma: Data collection, drafting of the manuscript, critical revision of intellectual content, and final approval of the manuscript; Ronald H. Borra: Data collection for logistics & workflow, implementation, challenges and future perspectives, drafting of the manuscript, critical revision of intellectual content, and final approval of the manuscript; Bart Cornelissen: Data collection for the preclinical oncology applications, drafting of the manuscript, and final approval of the manuscript; Rudi A. J. O. Dierckx: Data collection for clinical brain applications, drafting of the manuscript, and final approval of the manuscript; Magdalena Dobrolinska: Data collection for clinical cardiovascular applications, drafting of the manuscript, and final approval of the manuscript; Janine Doorduin: Data collection for preclinical brain applications, drafting of the manuscript, and final approval of the manuscript; Paola A. Erba: Data collection for challenges and future perspectives, drafting of the manuscript, and final approval of the manuscript; Andor W. J. M. Glaudemans: Data collection for clinical oncology applications, drafting of the manuscript, and final approval of the manuscript; Bruno Lima Giacobbo: Data collection for clinical brain applications, drafting of the manuscript, and final approval of the manuscript; Gert Luurtsema: Data collection for logistics & workflow, drafting of the manuscript, and final approval of the manuscript; Walter Noordzij: Data collection for clinical cardiovascular applications, drafting of the manuscript, and final approval of the manuscript; Joyce van Sluis: Data collection for clinical oncology applications, drafting of the manuscript, and final approval of the manuscript; Charalampos Tsoumpas: Conception and design of the work, data collection for the introduction, multitracer imaging, implementation, challenges and future perspectives, drafting of the manuscript, critical revision of intellectual content, and final approval of the manuscript; Adriaan A. Lammertsma: Conception and design of the work, data collection for the introduction, history drafting of the manuscript, critical revision of intellectual content, and final approval of the manuscript.

Declaration of Competing Interest

The authors declare that they have no known competing financial interests or personal relationships that could have appeared to influence the work reported in this paper.

References

1. Ter-Pogossian MM, Eichling JO, Davis DO, et al: The determination of regional cerebral blood flow by means of water labeled with radioactive oxygen 15. Radiology 93(1):31-40, 1969. https://doi.org/10.1148/93.1.31

2. Kanno I, Takahashi M, Yamaya T: Michel M. Ter-Pogossian (1925-1996): A pioneer of positron emission tomography weighted in fast imaging and Oxygen-15 application. Radiol Phys Technol 13(1):1-5, 2020. https://doi.org/10.1007/s12194-019-00549-z
3. Go KG, Lammertsma AA, Paans AM, et al: Extraction of water labeled with oxygen 15 during single-capillary transit. Influence of blood pressure, osmolarity, and blood-brain barrier damage. Arch Neurol 38(9):581-584, 1981. https://doi.org/10.1001/archneur.1981.00510090075009
4. Phelps ME, Hoffman EJ, Ter-Pogossian MM: Attenuation coefficients of various body tissues, fluids, and lesions at photon energies of 18 to 136 keV. Radiology 117(3 Pt 1):573-583, 1975. https://doi.org/10.1148/117.3.573
5. Phelps ME, Hoffman EJ, Huang SC, et al: ECAT: A new computerized tomographic imaging system for positron-emitting radiopharmaceuticals. J Nucl Med 19(6):635-647, 1978
6. Jones T, Chesler DA, Ter-Pogossian MM: The continuous inhalation of oxygen-15 for assessing regional oxygen extraction in the brain of man. Br J Radiol 49(580):339-343, 1976. https://doi.org/10.1259/0007-1285-49-580-339
7. West JB, Dollery CT: Uptake of oxygen-15-labeled CO2 compared with carbon-11-labeled CO2 in the lung. J Appl Physiol 17:9-13, 1962. https://doi.org/10.1152/jappl.1962.17.1.9
8. Frackowiak RS, Jones T, Lenzi GL, et al: Regional cerebral oxygen utilization and blood flow in normal man using oxygen-15 and positron emission tomography. Acta Neurol Scand 62(6):336-344, 1980. https://doi.org/10.1111/j.1600-0404.1980.tb03046.x
9. Herscovitch P, Markham J, Raichle ME: Brain blood flow measured with intravenous H2(15)O. I. Theory and error analysis. J Nucl Med 24(9):782-789, 1983
10. Raichle ME, Martin WR, Herscovitch P, et al: Brain blood flow measured with intravenous H2(15)O. II. Implementation and validation. J Nucl Med Sep 24(9):790-798, 1983
11. Kety SS: The theory and applications of the exchange of inert gas at the lungs and tissues. Pharmacol Rev Mar 3(1):1-41, 1951
12. Lammertsma AA, Frackowiak RS, Hoffman JM, et al: The C15O2 build-up technique to measure regional cerebral blood flow and volume of distribution of water. J Cereb Blood Flow Metab 9(4):461-470, 1989. https://doi.org/10.1038/jcbfm.1989.69
13. Raichle ME, Eichling JO, Straatmann MG, et al: Blood-brain-barrier permeability of C-11-labeled alcohols and O-15-labeled water. Am J Physiol 230(2):543-552, 1976. https://doi.org/10.1152/ajplegacy.1976.230.2.543
14. Clark JC, Buckingham PD: Short-Lived Radioactive Gases for Clinical Use. Butterworth's, 1975
15. Clark JC, Crouzel C, Meyer GJ, et al: Current methodology for O-15 production for clinical use. Appl Radiat Isotop 38(8):597-600, 1987. https://doi.org/10.1016/0883-2889(87)90122-5
16. Poetzsch S, Brenner W, Spreckelmeyer S: Are radiopharmaceuticals self- sterilizing? Radiation effect of gallium-68 and lutetium-177 on bacillus pumilus and staphylococcus succinus. Nuklearmedizin 60(06):445-449, 2021. https://doi.org/10.1055/a-1547-0628
17. Sipilä HT, Haaslahti V, Saunavaara V, et al: A PET/MR compatible device for production of Radiowater. In: Presented at: IEEE Nuclear Science Symposium and Medical Imaging Conference (NSS/MIC), Seattle, WA, 2014; Seattle, WA.
18. Pharma MA. First patient imaged with MedTrace technology. https://medtrace.dk/blog/first-patient-imaged-with-medtrace-technology/. Accessed 12 January 2021.
19. Wieland BW, Hendry GO, Schmidt DG: Design and performance of targets for producing C-11, N-13, O-15 and F-18 with 11 Mev protons. J Label Compd Radiopharm 23(10-12):1187-1189, 1986
20. Harms HJ, Nesterov SV, Han C, et al: Comparison of clinical non-commercial tools for automated quantification of myocardial blood flow using oxygen-15-labelled water PET/CT. Eur Heart J Cardiovasc Imaging 15(4):431-441, 2014. https://doi.org/10.1093/ehjci/jet177
21. Rainio O, Han C, Teuho J, et al: Carimas: An extensive medical imaging data processing tool for research. J Digit Imaging 36(4):1885-1893, 2023.. https://doi.org/10.1007/s10278-023-00812-1
22. Nordström J, Lindström E, Kero T, et al: Influence of image reconstruction on quantitative cardiac (15)O-water positron emission tomography. J Nucl Cardiol 30(2):716-725, 2023. https://doi.org/10.1007/s12350-022-03075-5
23. Choi JW, Budzevich M, Wang S, et al: In vivo positron emission tomographic blood pool imaging in an immunodeficient mouse model using 18F-fluorodeoxyglucose labeled human erythrocytes. PLoS One 14(1):e0211012. https://doi.org/10.1371/journal.pone.0211012, 2019
24. Ahnen M, Becker R, Buck A, et al: Performance measurements of the SAFIR prototype detector with the STiC ASIC readout. IEEE Trans Med Imaging 2(3):250-258, 2018. https://doi.org/10.1109/TRPMS.2018.2797484
25. Martin A, Mace E, Boisgard R, et al: Imaging of perfusion, angiogenesis, and tissue elasticity after stroke. J Cereb Blood Flow Metab 32(8):1496-1507, 2012. https://doi.org/10.1038/jcbfm.2012.49
26. Temma T, Kuge Y, Sano K, et al: PET O-15 cerebral blood flow and metabolism after acute stroke in spontaneously hypertensive rats. Brain Res 1212:18-24, 2008. https://doi.org/10.1016/j.brainres.2008.03.033
27. Urakami T, Kawaguchi AT, Akai S, et al: In vivo distribution of liposome-encapsulated hemoglobin determined by positron emission tomography. Artif Organs 33(2):164-168, 2009. https://doi.org/10.1111/j.1525-1594.2008.00702.x
28. Walberer M, Backes H, Rueger MA, et al: Potential of early [(18)F]-2-fluoro-2-deoxy-D-glucose positron emission tomography for identifying hypoperfusion and predicting fate of tissue in a rat embolic stroke model. Stroke 43(1):193-198, 2012. https://doi.org/10.1161/STROKEAHA.111.624551
29. Zwagerman N, Sprague S, Davis MD, et al: Pre-ischemic exercise preserves cerebral blood flow during reperfusion in stroke. Neurol Res 32(5):523-529, 2010. https://doi.org/10.1179/016164109X12581096796431
30. Endepols H, Mertgens H, Backes H, et al: Longitudinal assessment of infarct progression, brain metabolism and behavior following anterior cerebral artery occlusion in rats. J Neurosci Methods 253:279-291, 2015. https://doi.org/10.1016/j.jneumeth.2014.11.003
31. Wehrl HF, Martirosian P, Schick F, et al: Assessment of rodent brain activity using combined [(15)O]H_2O-PET and BOLD-fMRI. Neuroimage 89:271-279, 2014. https://doi.org/10.1016/j.neuroimage.2013.11.044
32. Gronman M, Tarkia M, Stark C, et al: Assessment of myocardial viability with [(15)O]water PET: A validation study in experimental myocardial infarction. J Nucl Cardiol 28(4):1271-1280, 2021. https://doi.org/10.1007/s12350-019-01818-5
33. Kudomi N, Sipila H, Autio A, et al: Cross-validation of input functions obtained by H(2) 15O PET imaging of rat heart and a blood flow-through detector. Mol Imaging Biol 14(4):509-516, 2012. https://doi.org/10.1007/s11307-011-0511-5
34. McFalls EO, Baldwin D, Marx D, et al: Temporal changes in function and regional glucose uptake within stunned porcine myocardium. J Nucl Med 37(12):2006-2010, 1996
35. Nielsen RR, Sorensen J, Tolbod L, et al: Quantitative estimation of extravascular lung water volume and preload by dynamic 15O-water positron emission tomography. Eur Heart J Cardiovasc Imaging 20(10):1120-1128, 2019. https://doi.org/10.1093/ehjci/jez038
36. Tarkia M, Stark C, Haavisto M, et al: Cardiac remodeling in a new pig model of chronic heart failure: Assessment of left ventricular functional, metabolic, and structural changes using PET, CT, and echocardiography. J Nucl Cardiol 22(4):655-665, 2015. https://doi.org/10.1007/s12350-015-0068-9
37. Watabe H, Jino H, Kawachi N, et al: Parametric imaging of myocardial blood flow with 15O-water and PET using the basis function method. J Nucl Med 46(7):1219-1224, 2005
38. Bol A, Melin JA, Vanoverschelde JL, et al: Direct comparison of [13N] ammonia and [15O]water estimates of perfusion with quantification of regional myocardial blood flow by microspheres. Circulation 87(2):512-525, 1993. https://doi.org/10.1161/01.cir.87.2.512
39. Manabe O, Kikuchi T, Scholte A, et al: Radiopharmaceutical tracers for cardiac imaging. J Nucl Cardiol 25(4):1204-1236, 2018. https://doi.org/10.1007/s12350-017-1131-5

40. de Langen AJ, van den Boogaart VE, Marcus JT, Lubberink M: Use of H2(15)O-PET and DCE-MRI to measure tumor blood flow. Oncologist 13(6):631-644, 2008. https://doi.org/10.1634/theoncologist.2007-0235
41. Bao A, Goins B, Dodd GD 3rd, et al: Real-time iterative monitoring of radiofrequency ablation tumor therapy with 15O-water PET imaging. J Nucl Med 49(10):1723-1729, 2008. https://doi.org/10.2967/jnumed.108.052886
42. Herrero P, Kim J, Sharp TL, et al: Assessment of myocardial blood flow using 15O-water and 1-11C-acetate in rats with small-animal PET. J Nucl Med 47(3):477-485, 2006
43. Autio A, Saraste A, Kudomi N, et al: Assessment of blood flow with (68)Ga-DOTA PET in experimental inflammation: A validation study using (15)O-water. Am J Nucl Med Mol Imaging 4(6):571-579, 2014
44. Mokhber N, Shariatzadeh A, Avan A, et al: Cerebral blood flow changes during aging process and in cognitive disorders: A review. Neuroradiol J 34(4):300-307, 2021. https://doi.org/10.1177/19714009211002778
45. Aanerud J, Borghammer P, Chakravarty MM, et al: Brain energy metabolism and blood flow differences in healthy aging. J Cereb Blood Flow Metab 32(7):1177-1187, 2012. https://doi.org/10.1038/jcbfm.2012.18
46. Bremmer JP, van Berckel BN, Persoon S, et al: Day-to-day test-retest variability of CBF, CMRO2, and OEF measurements using dynamic 15O PET studies. Mol Imaging Biol 13(4):759-768, 2011. https://doi.org/10.1007/s11307-010-0382-1
47. Scarmeas N, Zarahn E, Anderson KE, et al: Association of life activities with cerebral blood flow in Alzheimer disease: Implications for the cognitive reserve hypothesis. Arch Neurol 60(3):359-365, 2003. https://doi.org/10.1001/archneur.60.3.359
48. Xu G, Rowley HA, Wu G, et al: Reliability and precision of pseudo-continuous arterial spin labeling perfusion MRI on 3.0 T and comparison with 15O-water PET in elderly subjects at risk for Alzheimer's disease. NMR Biomed 23(3):286-293, 2010. https://doi.org/10.1002/nbm.1462
49. Hays CC, Zlatar ZZ, Wierenga CE: The utility of cerebral blood flow as a biomarker of preclinical Alzheimer's disease. Cell Mol Neurobiol 36(2):167-179, 2016. https://doi.org/10.1007/s10571-015-0261-z
50. Wierenga CE, Hays CC, Zlatar ZZ: Cerebral blood flow measured by arterial spin labeling MRI as a preclinical marker of Alzheimer's disease. J Alzheimers Dis 42(Suppl 4):S411-S419, 2014. https://doi.org/10.3233/Jad-141467
51. Bartenstein P, Weindl A, Spiegel S, et al: Central motor processing in Huntington's disease: A PET activation study. J Nucl Med 38(5), 1997. 387-387
52. Boecker H, Ceballos-Baumann A, Bartenstein P, et al: Sensory processing in Parkinson's and Huntington's disease: Investigations with 3D H(2)(15)O-PET. Brain 122(Pt 9):1651-1665, 1999. https://doi.org/10.1093/brain/122.9.1651
53. Pagano G, Niccolini F, Politis M: Current status of PET imaging in Huntington's disease. Eur J Nucl Med Mol Imaging 43(6):1171-1182, 2016. https://doi.org/10.1007/s00259-016-3324-6
54. Samuel M, Ceballos-Baumann AO, Blin J, et al: Evidence for lateral premotor and parietal overactivity in Parkinson's disease during sequential and bimanual movements. A PET study. Brain 120(Pt 6):963-976, 1997. https://doi.org/10.1093/brain/120.6.963
55. Dunn RT, Willis MW, Benson BE, et al: Preliminary findings of uncoupling of flow and metabolism in unipolar compared with bipolar affective illness and normal controls. Psychiatry Res 140(2):181-198, 2005. https://doi.org/10.1016/j.pscychresns.2005.07.005
56. Kim JJ, Park HJ, Jung YC, et al: Evaluative processing of ambivalent stimuli in patients with schizophrenia and depression: A [15O] H_2O PET study. J Int Neuropsychol Soc 15(6):990-1001, 2009. https://doi.org/10.1017/S1355617709990403
57. Conen S, Matthews JC, Patel NK, et al: Acute and chronic changes in brain activity with deep brain stimulation for refractory depression. J Psychopharmacol 32(4):430-440, 2018. https://doi.org/10.1177/0269881117742668
58. King AP, Abelson JL, Britton JC, et al: Medial prefrontal cortex and right insula activity predict plasma ACTH response to trauma recall. Neuroimage 47(3):872-880, 2009. https://doi.org/10.1016/j.neuroimage.2009.05.088
59. Liberzon I, King AP, Britton JC, et al: Paralimbic and medial prefrontal cortical involvement in neuroendocrine responses to traumatic stimuli. Am J Psychiatry 164(8):1250-1258, 2007. https://doi.org/10.1176/appi.ajp.2007.06081367
60. Phan KL, Britton JC, Taylor SF, et al: Corticolimbic blood flow during nontraumatic emotional processing in posttraumatic stress disorder. Arch Gen Psychiatry 63(2):184-192, 2006. https://doi.org/10.1001/archpsyc.63.2.184
61. Leenders KL, Perani D, Lammertsma AA, et al: Cerebral blood flow, blood volume and oxygen utilization. Normal values and effect of age. Brain 113(Pt 1):27-47, 1990. https://doi.org/10.1093/brain/113.1.27
62. Herholz K, Heiss WD: Positron emission tomography in clinical neurology. Mol Imaging Biol 6(4):239-269, 2004. https://doi.org/10.1016/j.mibio.2004.05.002
63. Sciagra R, Lubberink M, Hyafil F, et al: EANM procedural guidelines for PET/CT quantitative myocardial perfusion imaging. Eur J Nucl Med Mol Imaging 48(4):1040-1069, 2021. https://doi.org/10.1007/s00259-020-05046-9
64. Maaniitty T, Knuuti J, Saraste A: 15O-Water PET MPI: Current status and future perspectives. Semin Nucl Med 50(3):238-247, 2020. https://doi.org/10.1053/j.semnuclmed.2020.02.011
65. Harms HJ, Knaapen P, de Haan S, et al: Automatic generation of absolute myocardial blood flow images using [15O]H_2O and a clinical PET/CT scanner. Eur J Nucl Med Mol Imaging 38(5):930-939, 2011. https://doi.org/10.1007/s00259-011-1730-3
66. Danad I, Raijmakers PG, Driessen RS, et al: Comparison of coronary CT angiography, SPECT, PET, and hybrid imaging for diagnosis of ischemic heart disease determined by fractional flow reserve. JAMA Cardiol 2(10):1100-1107, 2017. https://doi.org/10.1001/jamacardio.2017.2471
67. Driessen RS, Bom MJ, van Diemen PA, et al: Incremental prognostic value of hybrid [15O]H_2O positron emission tomography-computed tomography: Combining myocardial blood flow, coronary stenosis severity, and high-risk plaque morphology. Eur Heart J Cardiovasc Imaging 21(10):1105-1113, 2020. https://doi.org/10.1093/ehjci/jeaa192
68. Driessen RS, Danad I, Stuijfzand WJ, et al: Impact of revascularization on absolute myocardial blood flow as assessed by serial [(15)O]H_2O positron emission tomography imaging: A comparison with fractional flow reserve. Circ Cardiovasc Imaging 11(5):e007417. https://doi.org/10.1161/CIRCIMAGING.117.007417, 2018
69. de Haan S, Harms HJ, Lubberink M, et al: Parametric imaging of myocardial viability using (1)(5)O-labelled water and PET/CT: Comparison with late gadolinium-enhanced CMR. Eur J Nucl Med Mol Imaging 39(8):1240-1245, 2012. https://doi.org/10.1007/s00259-012-2134-8
70. Naum A, Laaksonen MS, Tuunanen H, et al: Motion detection and correction for dynamic (15)O-water myocardial perfusion PET studies. Eur J Nucl Med Mol Imaging 32(12):1378-1383, 2005. https://doi.org/10.1007/s00259-005-1846-4
71. Kero T, Nordström J, Harms HJ, et al: Quantitative myocardial blood flow imaging with integrated time-of-flight PET-MR. EJNMMI Phys 4(1):1, 2017. https://doi.org/10.1186/s40658-016-0171-2
72. Nordstrom J, Kvernby S, Kero T, et al: Left-ventricular volumes and ejection fraction from cardiac ECG-gated (15)O-water positron emission tomography compared to cardiac magnetic resonance imaging using simultaneous hybrid PET/MR. J Nucl Cardiol 30(4):1352-1362, 2023. https://doi.org/10.1007/s12350-022-03154-7
73. Shabani Varaki E, Gargiulo GD, Penkala S, et al: Peripheral vascular disease assessment in the lower limb: A review of current and emerging non-invasive diagnostic methods. Biomed Eng Online 17(1):61, 2018. https://doi.org/10.1186/s12938-018-0494-4
74. Stacy MR, Zhou W, Sinusas AJ: Radiotracer imaging of peripheral vascular disease. J Nucl Med 54(12):2104-2110, 2013. https://doi.org/10.2967/jnumed.112.115105

75. Raitakari M, Nuutila P, Ruotsalainen U, et al: Relationship between limb and muscle blood flow in man. J Physiol 496(Pt 2):543-549, 1996. https://doi.org/10.1113/jphysiol.1996.sp021705
76. Ament W, Lubbers J, Rakhorst G, et al: Skeletal muscle perfusion measured by positron emission tomography during exercise. Pflugers Arch 436(5):653-658, 1998. https://doi.org/10.1007/s004240050685
77. Schmidt MA, Chakrabarti A, Shamim-Uzzaman Q, et al: Calf flow reserve with H(2)(15)O PET as a quantifiable index of lower extremity flow. J Nucl Med 44(6):915-919, 2003
78. Scremin OU, Figoni SF, Norman K, et al: Preamputation evaluation of lower-limb skeletal muscle perfusion with H(2) (15)O positron emission tomography. Am J Phys Med Rehabil 89(6):473-486, 2010. https://doi.org/10.1097/PHM.0b013e3181d89b08
79. Kalliokoski KK, Knuuti J, Nuutila P: Relationship between muscle blood flow and oxygen uptake during exercise in endurance-trained and untrained men. J Appl Physiol (1985) 98(1):380-383, 2005. https://doi.org/10.1152/japplphysiol.01306.2003
80. Nuutila P, Kalliokoski K: Use of positron emission tomography in the assessment of skeletal muscle and tendon metabolism and perfusion. Scand J Med Sci Sports 10(6):346-350, 2000. https://doi.org/10.1034/j.1600-0838.2000.010006346.x
81. Taniguch H, Kunishima S, Koh T, et al: Reproducibility of repeated human regional splenic blood flow measurements using [15O] water and positron emission tomography. Nucl Med Commun 22(7):755-757, 2001. https://doi.org/10.1097/00006231-200107000-00005
82. Kudomi N, Slimani L, Jarvisalo MJ, et al: Non-invasive estimation of hepatic blood perfusion from H2 15O PET images using tissue-derived arterial and portal input functions. Eur J Nucl Med Mol Imaging 35(10):1899-1911, 2008. https://doi.org/10.1007/s00259-008-0796-z
83. Ziegler SI, Haberkorn U, Byrne H, et al: Measurement of liver blood flow using oxygen-15 labelled water and dynamic positron emission tomography: Limitations of model description. Eur J Nucl Med 23 (2):169-177, 1996. https://doi.org/10.1007/BF01731841
84. Virtanen KA, Peltoniemi P, Marjamaki P, et al: Human adipose tissue glucose uptake determined using [(18)F]-fluoro-deoxy-glucose ([(18) F]FDG) and PET in combination with microdialysis. Diabetologia 44 (12):2171-2179, 2001. https://doi.org/10.1007/s001250100026
85. Viljanen AP, Virtanen KA, Jarvisalo MJ, et al: Rosiglitazone treatment increases subcutaneous adipose tissue glucose uptake in parallel with perfusion in patients with type 2 diabetes: A double-blind, randomized study with metformin. J Clin Endocrinol Metab 90(12):6523-6528, 2005. https://doi.org/10.1210/jc.2005-1073
86. Lahesmaa M, Oikonen V, Helin S, et al: Regulation of human brown adipose tissue by adenosine and A2A receptors—studies with [(15)O] H_2O and [(11)C]TMSX PET/CT. Eur J Nucl Med Mol Imaging. Mar 46 (3):743-750, 2019. https://doi.org/10.1007/s00259-018-4120-2
87. Ito M, Lammertsma AA, Wise RJ, et al: Measurement of regional cerebral blood flow and oxygen utilisation in patients with cerebral tumours using 15O and positron emission tomography: Analytical techniques and preliminary results. Neuroradiology 23(2):63-74, 1982. https://doi.org/10.1007/BF00367239
88. Beaney RP, Lammertsma AA, Jones T, et al: Positron emission tomography for in-vivo measurement of regional blood flow, oxygen utilisation, and blood volume in patients with breast carcinoma. Lancet 1 (8369):131-134, 1984. https://doi.org/10.1016/s0140-6736(84)90063-1
89. Lopes-Coelho F, Martins F, Pereira SA, et al: Anti-angiogenic therapy: Current challenges and future perspectives. Int J Mol Sci 22(7):3765, 2021. https://doi.org/10.3390/ijms22073765
90. van der Veldt AA, Hendrikse NH, Harms HJ, et al: Quantitative parametric perfusion images using 15O-labeled water and a clinical PET/CT scanner: Test-retest variability in lung cancer. J Nucl Med 51 (11):1684-1690, 2010. https://doi.org/10.2967/jnumed.110.079137
91. de Langen AJ, van den Boogaart V, Lubberink M, et al: Monitoring response to antiangiogenic therapy in non-small cell lung cancer using imaging markers derived from PET and dynamic contrast-enhanced MRI. J Nucl Med 52(1):48-55, 2011. https://doi.org/10.2967/jnumed.110.078261
92. Scott AM, Mitchell PL, O'Keefe G, et al: Pharmacodynamic analysis of tumour perfusion assessed by 15O-water-PET imaging during treatment with sunitinib malate in patients with advanced malignancies. EJNMMI Res 2(1):31, 2012. https://doi.org/10.1186/2191-219X-2-31
93. Lubberink M, Golla SS, Jonasson M, et al: (15)O-water PET study of the effect of imatinib, a selective platelet-derived growth factor receptor inhibitor, versus anakinra, an IL-1R antagonist, on water-perfusable tissue fraction in colorectal cancer metastases. J Nucl Med 56(8):1144-1149, 2015. https://doi.org/10.2967/jnumed.114.151894
94. Krak N, van der Hoeven J, Hoekstra O, et al: Blood flow and glucose metabolism in stage IV breast cancer: Heterogeneity of response during chemotherapy. Mol Imaging Biol 10(6):356-363, 2008. https://doi.org/10.1007/s11307-008-0163-2
95. Specht JM, Kurland BF, Montgomery SK, et al: Tumor metabolism and blood flow as assessed by positron emission tomography varies by tumor subtype in locally advanced breast cancer. Clin Cancer Res 16(10):2803-2810, 2010. https://doi.org/10.1158/1078-0432.CCR-10-0026
96. Lehtio K, Oikonen V, Gronroos T, et al: Imaging of blood flow and hypoxia in head and neck cancer: Initial evaluation with [(15)O]H(2)O and [(18)F]fluoroerythronitroimidazole PET. J Nucl Med. Nov 42 (11):1643-1652, 2001
97. Tolbod LP, Nielsen MM, Pedersen BG, et al: Non-invasive quantification of tumor blood flow in prostate cancer using (15)O-H_2O PET/CT. Am J Nucl Med Mol Imaging 8(5):292-302, 2018
98. Bruehlmeier M, Roelcke U, Schubiger PA, et al: Assessment of hypoxia and perfusion in human brain tumors using PET with 18F-fluoromisonidazole and 15O-H_2O. J Nucl Med 45(11):1851-1859, 2004
99. Van der Veldt AA, Lubberink M, Bahce I, et al: Rapid decrease in delivery of chemotherapy to tumors after anti-VEGF therapy: Implications for scheduling of anti-angiogenic drugs. Cancer Cell 21(1):82-91, 2012. https://doi.org/10.1016/j.ccr.2011.11.023
100. Lodge MA, Carson RE, Carrasquillo JA, et al: Parametric images of blood flow in oncology PET studies using [15O]water. J Nucl Med. Nov 41(11):1784-1792, 2000
101. Lodge MA, Jacene HA, Pili R, et al: Reproducibility of tumor blood flow quantification with 15O-water PET. J Nucl Med 49(10):1620-1627, 2008. https://doi.org/10.2967/jnumed.108.052076
102. Slart R, Tsoumpas C, Glaudemans A, et al: Long axial field of view PET scanners: A road map to implementation and new possibilities. Eur J Nucl Med Mol Imaging 48(13):4236-4245, 2021. https://doi.org/10.1007/s00259-021-05461-6
103. Healthineers S. Multiparametric PET AI. https://www.siemens-healthineers.com/nl/molecular-imaging/options-and-upgrades/software-applications/flowmotion-multiparametricpet-suite
104. Pantel AR, Viswanath V, Daube-Witherspoon ME, et al: PennPET explorer: Human imaging on a whole-body imager. J Nucl Med 61 (1):144-151, 2020. https://doi.org/10.2967/jnumed.119.231845
105. Prenosil GA, Sari H, Furstner M, et al: Performance characteristics of the biograph vision quadra PET/CT system with a long axial field of view using the NEMA NU 2-2018 standard. J Nucl Med 63(3):476-484, 2022. https://doi.org/10.2967/jnumed.121.261972
106. Spencer BA, Berg E, Schmall JP, et al: Performance evaluation of the uEXPLORER total-body PET/CT scanner based on NEMA NU 2-2018 with additional tests to characterize PET scanners with a long axial field of view. J Nucl Med 62(6):861-870, 2021. https://doi.org/10.2967/jnumed.120.250597
107. Iida H, Miura S, Shoji Y, et al: Noninvasive quantitation of cerebral blood flowusing oxygen-15-water and a dual-PET system. J Nucl Med 39(10):1789-1798, 1998
108. Dagogo-Jack I, Shaw AT: Tumour heterogeneity and resistance to cancer therapies. Nat Rev Clin Oncol 15(2):81-94, 2018. https://doi.org/10.1038/nrclinonc.2017.166
109. Iozzo P, Chareonthaitawee P, Di Terlizzi M, et al: Regional myocardial blood flow and glucose utilization during fasting and physiological hyperinsulinemia in humans. Am J Physiol Endocrinol Metab 282(5): E1163-E1171, 2002. https://doi.org/10.1152/ajpendo.00386.2001
110. Verhaeghe J, Reader AJ: Simultaneous water activation and glucose metabolic rate imaging with PET. Phys Med Biol 58(3):393-411, 2013. https://doi.org/10.1088/0031-9155/58/3/393

111. Smith T, Tong C, Lammertsma AA, et al: Dosimetry of intravenously administered oxygen-15 labelled water in man: A model based on experimental human data from 21 subjects. Eur J Nucl Med 21 (10):1126-1134, 1994. https://doi.org/10.1007/bf00181069
112. Alberts I, Hunermund JN, Prenosil G, et al: Clinical performance of long axial field of view PET/CT: A head-to-head intra-individual comparison of the biograph vision quadra with the biograph vision PET/CT. Eur J Nucl Med Mol Imaging 48(8):2395-2404, 2021. https://doi.org/10.1007/s00259-021-05282-7
113. Woods M, Brehm M. White Paper: Shaping the Beam. Versatile filtration for unique diagnostic potential within Siemens Healthineers CT. Siemens Healthineers Headquarters. 2019;
114. Jones T, Budinger TF: The potential for low-dose functional studies in maternal-fetal medicine using PET/MR imaging. J Nucl Med 54 (11):2016-2017, 2013. https://doi.org/10.2967/jnumed.113.123919
115. Kuttner S, Wickstrøm KK, Lubberink M, et al: Cerebral blood flow measurements with (15)O-water PET using a non-invasive machine-learning-derived arterial input function. J Cereb Blood Flow Metab 41 (9):2229-2241, 2021. https://doi.org/10.1177/0271678x21991393
116. Bertolli O, Eleftheriou A, Cecchetti M, et al: PET iterative reconstruction incorporating an efficient positron range correction method. Phys Med 32(2):323-330, 2016. https://doi.org/10.1016/j.ejmp.2015.11.005
117. Deidda D, Karakatsanis N, Robson P, et al: Hybrid PET-MR list-mode kernelized expectation maximization reconstruction. Inverse Problems 39:1-24, 2019
118. Polycarpou I, Soultanidis G, Tsoumpas C: Synergistic motion compensation strategies for positron emission tomography when acquired simultaneously with magnetic resonance imaging. Philos Trans A Math Phys Eng Sci 379(2204):20200207. https://doi.org/10.1098/rsta.2020.0207, 2021